AMERICAN SOCIETY FOR MICROBIOLOGY | Infection and Immunity®

FUNGAL AND PARASITIC INFECTIONS

Tumor Necrosis Factor Alpha Antagonism Reveals a Gut/Lung Axis That Amplifies Regulatory T Cells in a Pulmonary Fungal Infection

Jamie L. Tweedle,[a,b] George S. Deepe, Jr.[a,c]

[a]Division of Infectious Diseases, College of Medicine, University of Cincinnati, Cincinnati, Ohio, USA

[b]Program of Pathobiology and Molecular Medicine, College of Medicine, University of Cincinnati, Cincinnati, Ohio, USA

[c]Veterans Affairs Hospital, Cincinnati, Ohio, USA

ABSTRACT Tumor necrosis factor (TNF) antagonists are popular therapies for inflammatory diseases. These agents enhance the numbers and function of regulatory T cells (Tregs), which are important in controlling inflammatory diseases. However, elevated Treg levels increase susceptibility to infections, including histoplasmosis. We determined the mechanism by which Tregs expand in TNF-neutralized mice infected with *Histoplasma capsulatum*. Lung CD11c$^+$ CD11b$^+$ dendritic cells (DCs), but not alveolar macrophages, from *H. capsulatum*-infected mice treated with anti-TNF induced a higher percentage of Tregs than control DCs *in vitro*. CD11b$^+$ CD103$^+$ DCs, understood to be unique to the intestines, were augmented in lungs with anti-TNF treatment. In the absence of this subset, DCs from anti-TNF-treated mice failed to amplify Tregs *in vitro*. CD11b$^+$ CD103$^+$ DCs from TNF-neutralized mice displayed higher retinaldehyde dehydrogenase 2 (RALDH2) gene expression, and CD11b$^+$ CD103$^+$ RALDH$^+$ DCs exhibited greater enzyme activity. To determine if CD11b$^+$ CD103$^+$ DCs migrated from gut to lung, fluorescent beads were delivered to the gut via oral gavage, and the lungs were assessed for bead-containing DCs. Anti-TNF induced migration of CD11b$^+$ CD103$^+$ DCs from the gut to the lung that enhanced the generation of Tregs in *H. capsulatum*-infected mice. Therefore, TNF neutralization promotes susceptibility to pulmonary *H. capsulatum* infection by promoting a gut/lung migration of DCs that enhances Tregs.

KEYWORDS dendritic cell, lung, fungus, anti-TNF, imaging flow cytometry, dendritic cells, intracellular fungi, lung infection, rodent, tumor necrosis factor

Tumor necrosis factor alpha (TNF) is a fundamental cytokine in mounting an immune response; however, high levels are detrimental and emerge in inflammatory diseases, including Crohn's disease, rheumatoid arthritis, and plaque psoriasis. TNF antagonists are commonly used to treat these diseases and exert their effects by enhancing the numbers and function of regulatory T cells (Tregs). Patients display compromised numbers and functions of Tregs, and those who respond to anti-TNF therapy exhibit increased numbers of circulating Tregs and restored Treg suppressive activity. A disadvantage of TNF neutralization is that it leads to increased susceptibility to infections, including fungal infections.

Histoplasmosis, caused by the dimorphic fungus *Histoplasma capsulatum*, is the most common fungal infection arising in patients receiving TNF antagonists (1). *H. capsulatum* exists in soil throughout the world but is endemic to the Mississippi River and Ohio River valleys in the United States. Immunocompetent people generally clear pulmonary infection with minimal symptoms; however, immunocompromised individuals can develop severe, life-threatening disseminated disease. Clearance of the fungus

Received 5 February 2018 **Returned for modification** 25 February 2018 **Accepted** 21 March 2018

Accepted manuscript posted online 26 March 2018

Citation Tweedle JL, Deepe GS, Jr. 2018. Tumor necrosis factor alpha antagonism reveals a gut/lung axis that amplifies regulatory T cells in a pulmonary fungal infection. Infect Immun 86: e00109-18. https://doi.org/10.1128/IAI.00109-18.

Editor Andreas J. Bäumler, University of California, Davis

Address correspondence to George S. Deepe, Jr., george.deepe@uc.edu.

hinges on successfully mounting a Th1 response. TNF neutralization disrupts the coordination between the innate and adaptive immune systems and prompts vulnerability to *H. capsulatum* infection in both mice and humans (2, 3). Mice treated with anti-TNF manifest higher fungal burdens and succumb to *H. capsulatum* infection (3). The dampened immune response is preceded by an amplification of Tregs beginning at day 4 postinfection (p.i.) in the lungs and day 7 p.i. in the lymph nodes (4, 5). Elimination of Tregs in TNF-neutralized mice rescues the mice from succumbing to *H. capsulatum* infection (4), thus highlighting the power of this cell population to stifle protective immunity.

Dendritic cells (DCs) are the bridge between the innate and adaptive immune systems. They present antigen to T cells to activate a T cell response. In the lungs, conventional $CD11c^+$ DCs (cDCs) are divided into two subsets: $CD11b^-$ $CD103^+$ (cDC1s) and $CD11b^+$ $CD103^-$ (cDC2s) (6, 7). cDC1s require the transcription factors Batf3 and IRF8 for differentiation and survival and best present antigen to $CD8^+$ T cells (8–14). cDC2s express IRF4 and are specialized at interacting with $CD4^+$ T cells to promote helper T cells or Tregs (15–25). A third population of cDCs is found in the intestines: $CD11b^+$ $CD103^+$ cDC2s. These migratory DCs are dependent on IRF4 and Notch2 and induce peripherally derived Tregs by secreting transforming growth factor β (TGF-β) and retinoic acid (16, 26–28). However, the role of $CD11b^+$ $CD103^+$ DCs outside the intestine remains obscure.

Utilizing a murine model of pulmonary histoplasmosis, we sought to determine the mechanism for elevated Treg levels with TNF antagonism in *H. capsulatum*-infected mice. We report that TNF neutralization during *H. capsulatum* infection causes DC-mediated Treg amplification, which prevents clearance of the fungus. Furthermore, we show that the $CD11b^+$ $CD103^+$ DCs responsible for inducing Tregs are recruited from the gut to the lung. These results demonstrate that TNF is critical in maintaining homeostasis and that the absence of TNF leads to dysregulation of lung and gut immunity.

RESULTS

Amplified Tregs with TNF antagonism in Foxp3-GFP mice. Previously, we have shown that mice infected with *H. capsulatum* and treated with anti-TNF display increased lung Tregs, characterized as $CD4^+$ $CD25^+$, as early as 4 days p.i (3). Recent studies have shown the transcription factor Forkhead box P3 (Foxp3) to be a master regulator for this lineage and an important marker for Tregs (29–31). Therefore, Foxp3-green fluorescent protein (GFP) mice were used to assess Tregs by fluorescence-activated cell sorting (FACS). Anti-TNF-treated mice infected intranasally (i.n.) with *H. capsulatum* displayed a higher percentage and cell number proportion of Tregs in the lungs as early as 4 days p.i. (Fig. 1A, B, and C; see Fig. S1 in the supplemental material). Thus, the use of Foxp3-GFP reporter mice recapitulated the original findings and serves as a model for characterizing Tregs.

Stability of Foxp3 expression promotes Treg suppressor activity (32). The Foxp3 mean fluorescent intensity (MFI) in Tregs from anti-TNF-treated mice was increased compared to control mice (Fig. 1D and E). This suggests the suppressor activity of Tregs is superior in the absence of TNF. This finding agrees with previous work showing that TNF antagonism not only increases the numbers of these cells, but augments suppressor activity (33).

The Ikaros family transcription factor Helios has been described as a marker for natural Tregs as opposed to peripheral Tregs (34). To determine whether the increased Tregs were thymically or peripherally derived, $CD4^+$ $CD25^+$ $Foxp3^+$ Tregs were sorted from the lungs of day 4 p.i. mice treated with isotype control antibody or anti-TNF. The expression level of Helios was decreased in Tregs from anti-TNF-treated mice compared to control mice (Fig. 1F), indicating the increased Tregs are peripherally derived.

DCs, but not alveolar macrophages, expand Tregs with TNF neutralization. In the lungs, DCs and alveolar macrophages independently induce differentiation and expansion of Tregs (35–37). To elucidate which population of cells is responsible for the

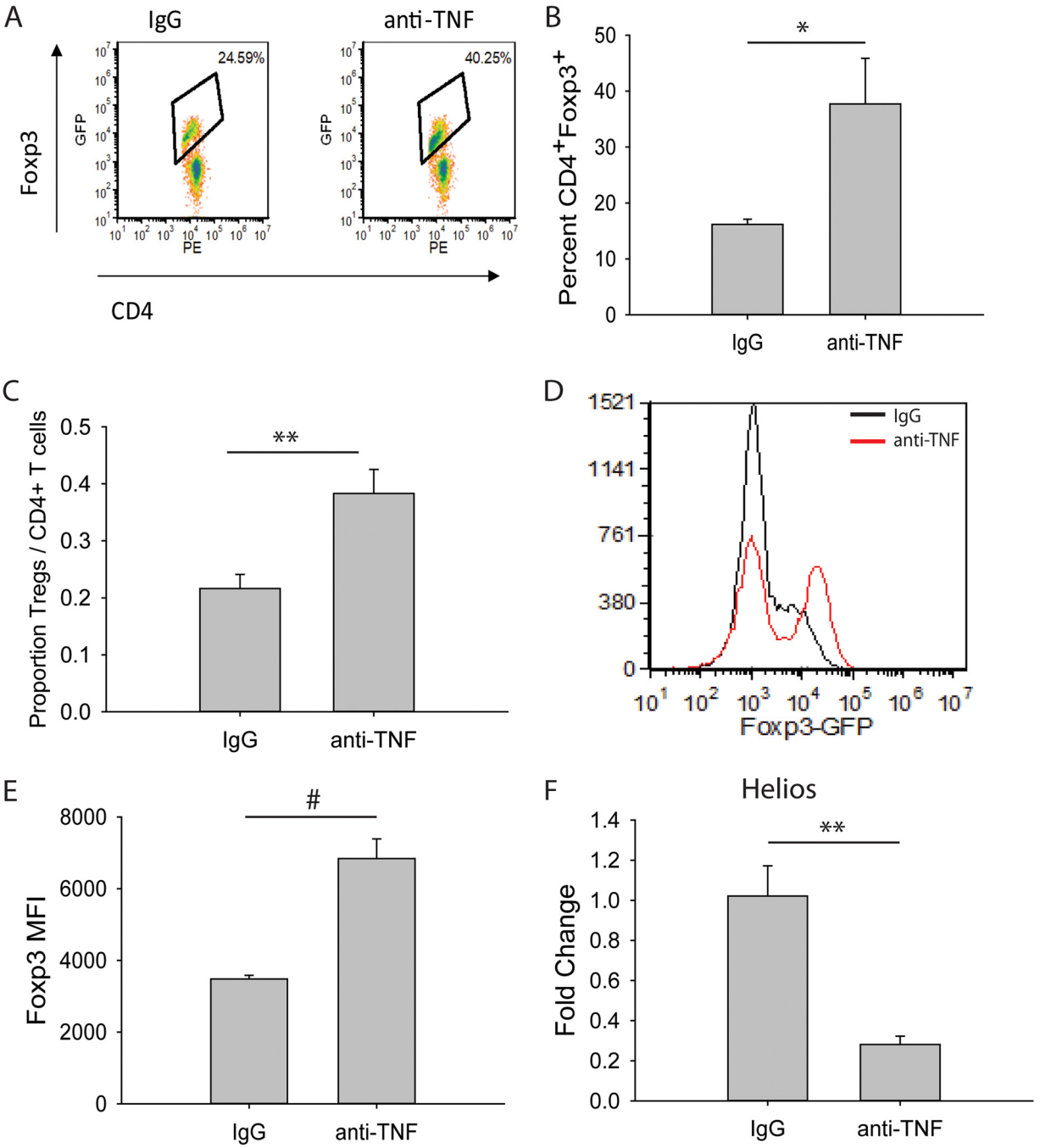

FIG 1 TNF antagonism induces increased Treg levels in *H. capsulatum*-infected mice. Foxp3-GFP mice were infected with 2×10^6 *H. capsulatum* yeasts i.n. and treated with anti-TNF or isotype control antibody. Lungs were harvested at day 4 p.i. and assessed for Tregs via flow cytometry. (A) Representative density plots of $CD4^+$ $CD25^+$ $Foxp3^+$ T cells. Cells demarcated by the diamonds represent $CD4^+$ $CD25^+$ $Foxp3^+$ Tregs. (B) Percentages of $CD4^+$ $CD25^+$ $Foxp3^+$ T cells. (C) Cell number proportions of $CD3^+$ $CD4^+$ $CD25^+$ $Foxp3^+$ Tregs to total $CD3^+$ $CD4^+$ T lymphocytes. (D) Representative histograms of Foxp3 MFI. (E) MFI of Foxp3 gated on $CD4^+$ $CD25^+$ cells. (F) $CD4^+$ $CD25^+$ $Foxp3^+$ Tregs were sorted from day 4 p.i. lungs, and RNA was extracted. Helios gene expression was assessed by qRT-PCR. The data represent means and standard errors of the mean (SEM) (n = 4 to 8 mice/group; representative of the results of at least two experiments). *, $P < 0.05$; **, $P < 0.01$; #, $P < 0.001$.

amplification of Tregs with TNF antagonism, DCs ($CD11c^+$ $CD11b^+$ major histocompatibility complex class II^+ [MHC-II^+]) and alveolar macrophages ($CD11c^+$ $CD11b^-$ $F4/80^+$) were assessed by FACS from the lungs of day 3 p.i. mice treated with anti-TNF or isotype control antibody. These cells were cocultured with splenic $CD4^+$ $CD25^-$ $Foxp3^-$ T cells from uninfected Foxp3-GFP mice. DCs, but not alveolar macrophages, from anti-TNF-treated mice generated higher percentages of Tregs than control mice

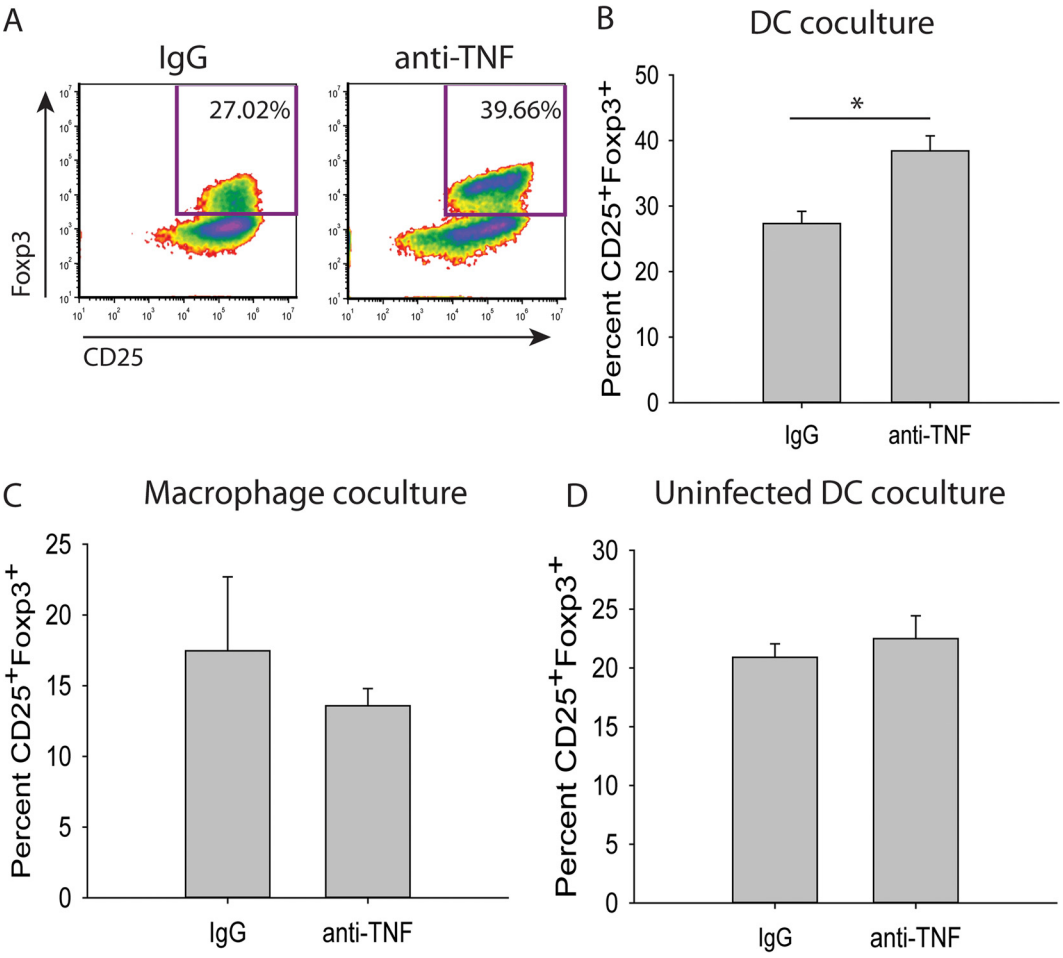

FIG 2 DCs from anti-TNF-treated *H. capsulatum*-infected mice amplify Tregs. (A to C) Mice were infected with 2×10^6 *H. capsulatum* yeasts i.n. and treated with anti-TNF or isotype control antibody. Lungs were harvested at day 3 p.i., and DCs ($CD11c^+$ $CD11b^+$ MHC-II^+) (A and B) and alveolar macrophages ($CD11c^+$ $CD11b^-$ $F4/80^+$) (C) were assessed by FACS. The cells were cocultured with splenic $CD4^+$ $CD25^-$ $Foxp3^-$ T cells from uninfected Foxp3-GFP mice in the presence of 1 μg/ml anti-CD3, 5 μg/ml anti-CD28, 3 ng/ml TGF-β, and 5 ng/ml IL-2. (D) Mice were treated with anti-TNF or isotype control antibody. Lungs were harvested 3 days after treatment, and DCs ($CD11c^+$ $CD11b^+$ MHC-II^+) were assessed by FACS. The cells were cocultured as described above. The data represent means and SEM of the results of at least 3 experiments. Lungs of 4 to 8 mice were pooled for each experiment. *, $P < 0.05$.

(Fig. 2A, B, and C). This expansion was a consequence of concurrent *H. capsulatum* infection and TNF antagonism, as it did not occur in coculture with DCs from uninfected mice (Fig. 2D).

TNF neutralization requires $CD11b^+$ $CD103^+$ DCs for Treg amplification. DCs comprise a heterogeneous population, and several subpopulations are known to expand Tregs in the periphery, including $CD103^+$, $CD11b^+$ $CD103^+$, PD-$L1^+$, and PD-$L2^+$ DCs (27, 28, 38–40). To determine if any of these populations were elevated with TNF antagonism, mice were infected with *H. capsulatum* and treated with anti-TNF or isotype control antibody, and at day 3 p.i., their lungs were assessed for Treg-inducing DC populations by flow cytometry. Anti-TNF-treated mice displayed an elevation in the percentage of $CD11b^+$ $CD103^+$ DCs, but the cell number was decreased (Fig. 3A and B; see Fig. S2 in the supplemental material). However, the percentage of total $CD11c^+$ $CD11b^+$ MHC-II^+ DCs was reduced in the lungs of anti-TNF-treated mice (Fig. 3C); thus, the ratio of $CD11b^+$ $CD103^+$ DCs to $CD11c^+$ $CD11b^+$ DCs was increased in the anti-TNF-treated mice (Fig. 3D). The modulation in $CD11b^+$ $CD103^+$ DCs was not caused by increased inoculum size (Fig. 3E), anti-TNF treatment in the absence of infection (Fig. 3F), or neutralization of interferon gamma (IFN-γ), another critical pro-

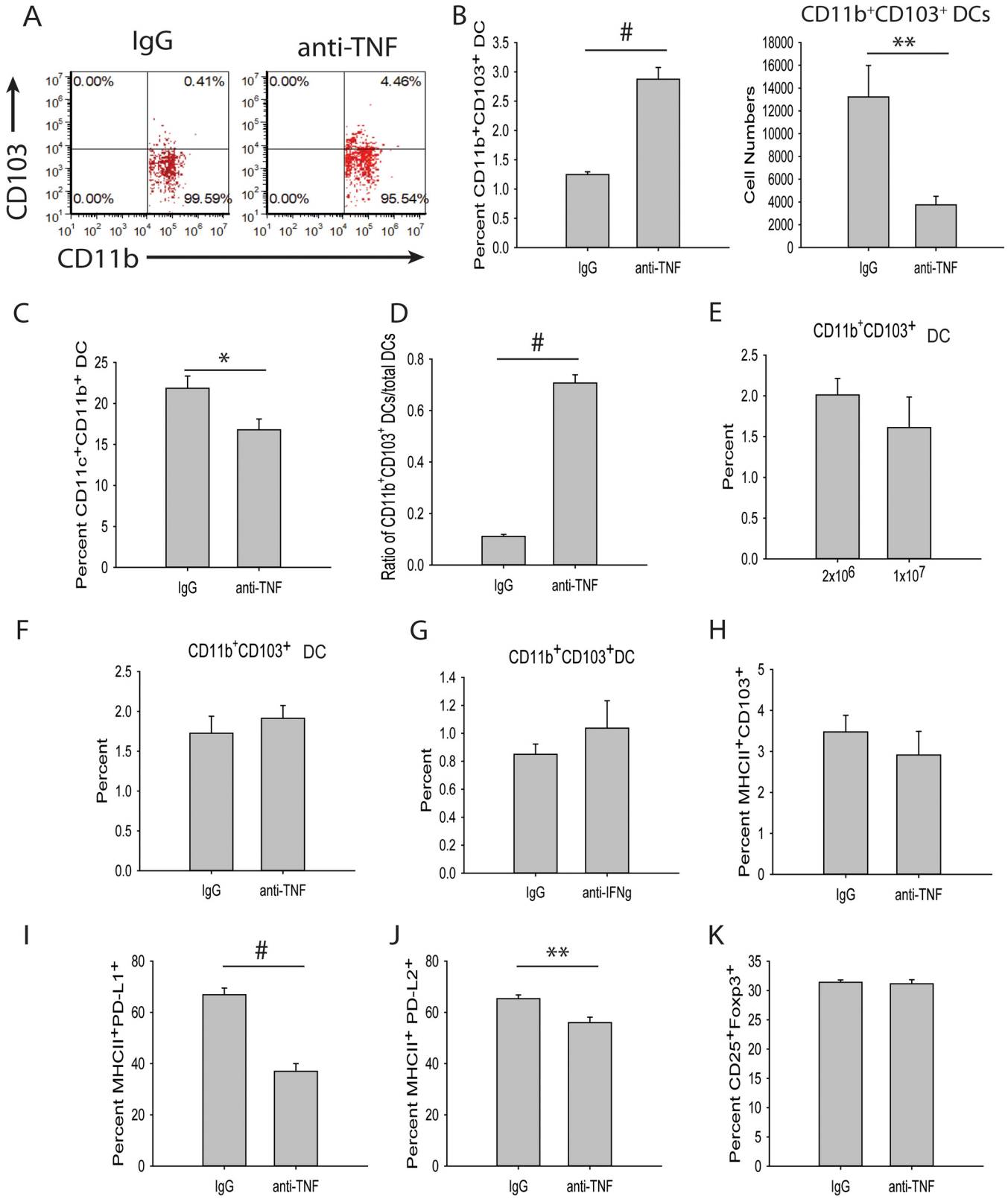

FIG 3 CD11b$^+$ CD103$^+$ DCs induce Tregs. (A to D) Mice were infected with 2×10^6 *H. capsulatum* yeasts i.n. and treated with anti-TNF or isotype control antibody. Lungs were harvested at day 3 p.i. and assessed for DC populations by FACS. The DCs were gated on CD11c$^+$ CD11b$^+$ MHC-II$^+$. (E) Mice were infected with 2×10^6 or 1×10^7 *H. capsulatum* yeasts i.n. Lungs were harvested at day 3 p.i., and DCs were assessed by FACS. (F and G) Mice were treated with anti-TNF (F), anti-IFN-γ (G), or isotype control antibody. Lungs were harvested 3 days after treatment, and DCs were assessed by FACS. The data represent means and SEM ($n = 8$ mice/group; representative of the results of two experiments). (H to J) Mice were infected with 2×10^6 *H. capsulatum* yeasts i.n. and treated with anti-TNF or isotype control antibody. Lungs were harvested at day 3 p.i. and assessed for DC populations by FACS. The DCs were first gated on CD11c$^+$ MHC-II$^+$.

(Continued on next page)

inflammatory cytokine promoting clearance of *H. capsulatum* (Fig. 3G) (41). The percentages of CD103$^+$ DCs and decreased PD-L1$^+$ and PD-L2$^+$ DCs were unchanged (Fig. 3H, I, and J; see Fig. S3 in the supplemental material).

To ascertain if TNF antagonism required the CD11b$^+$ CD103$^+$ DC population for the augmentation of Tregs, DCs were cocultured with T cells in the absence of CD11b$^+$ CD103$^+$ DCs. CD11c$^+$ CD11b$^+$ MHC-II$^+$ CD103$^-$ DCs were assessed by FACS from day 3 p.i. mice treated with anti-TNF or isotype control antibody and cocultured with splenic CD4$^+$ CD25$^-$ Foxp3$^-$ T cells from uninfected Foxp3-GFP mice. In the absence of the CD11b$^+$ CD103$^+$ DC population, expansion of Tregs was not observed (Fig. 3K). Therefore, the CD11b$^+$ CD103$^+$ DC population was responsible for the elevated Tregs with TNF antagonism.

CD11b$^+$ CD103$^+$ DCs have increased RALDH2 expression and aldehyde dehydrogenase activity, but not TGF-β. CD11b$^+$ CD103$^+$ DCs generate Tregs by secreting TGF-β and retinoic acid (27, 28, 42). While no differences were found in whole-lung TGF-β protein or CD11b$^+$ CD103$^+$ DC gene expression (Fig. 4A and B), the expression level of the retinoic acid-producing enzyme retinaldehyde dehydrogenase 2 (RALDH2) was amplified in total DCs and CD11b$^+$ CD103$^+$ DCs from the lungs of *H. capsulatum*-infected, anti-TNF-treated mice compared to control mice (Fig. 4C and D). RALDH2 activity was measured using an Aldefluor kit (Stem Cell Technologies, Vancouver, BC, Canada) and flow cytometry. The CD11b$^+$ CD103$^+$ Aldefluor$^+$ DC population from the lungs of *H. capsulatum*-infected, anti-TNF-treated mice had a higher MFI than the CD11b$^+$ CD103$^+$ Aldefluor$^+$ DC population from control mice (Fig. 4E), suggesting CD11b$^+$ CD103$^+$ DCs rely on increased retinoic acid but not enhanced TGF-β to induce Tregs in *H. capsulatum*-infected mice treated with anti-TNF.

CD11b$^+$ CD103$^+$ DCs migrate from gut to lung. The CD11b$^+$ CD103$^+$ DC population is unique to the intestines (11), prompting the hypothesis that CD11b$^+$ CD103$^+$ DCs migrate from gut to lung in *H. capsulatum*-infected mice treated with TNF antagonist. To investigate this hypothesis, we used two different approaches. First, fluorescently labeled *H. capsulatum* was used as a surrogate label for cells in the gut. Tandem dimeric Tomato (tdTomato)-*H. capsulatum* was delivered via oral gavage to *H. capsulatum*-infected and anti-TNF- or isotype control antibody-treated mice. Three days after i.n. infection, the lungs and intestines were collected to assess for fluorescent *H. capsulatum*. Confocal images established the presence of tdTomato-*H. capsulatum* in the lungs 3 days after oral gavage (Fig. 5A). Employing Amnis ImagestreamX (Millipore, Billerica, MA) to characterize cells with imaging flow cytometry, CD11b$^+$ CD103$^+$ DCs containing fluorescent *H. capsulatum* were identified in the lungs 3 days p.i. (Fig. 5B), indicating the cells migrated from the intestine to the lungs. However, due to concern that the oral gavage of fluorescently labeled *H. capsulatum* increased the overall fungal burden in the mice, we implemented a second method.

The same experiment was repeated using fluorescently labeled beads to address the concern over increased fungal burden. The mice were infected with *H. capsulatum*, treated with anti-TNF or isotype control antibody, and gavaged daily with fluorescently labeled beads. The lungs were collected at day 3 p.i. and analyzed using Amnis ImagestreamX. As a control, mice were given an i.n. dose of 2×10^6 beads, and lungs were collected 3 days later and analyzed using imaging flow cytometry (Fig. 5C and D). Cells containing fluorescently labeled beads were present in the lungs (Fig. 5E), and anti-TNF-treated mice harbored higher percentages, but not numbers, of bead-containing CD11b$^+$ CD103$^+$ cells (Fig. 5F, G, and H). Therefore, these data suggest CD11b$^+$ CD103$^+$ DCs migrate from gut to lung when TNF is neutralized in *H. capsulatum* infection.

FIG 3 Legend (Continued)

(I) Mice were infected with 2×10^6 *H. capsulatum* yeasts i.n. and treated with anti-TNF or isotype control antibody. Lungs were harvested at day 3 p.i., and CD11c$^+$ CD11b$^+$ MHC-II$^+$ CD103$^-$ DCs were assessed by FACS. Cells were cocultured with splenic CD4$^+$ CD25$^-$ Foxp3$^-$ T cells from uninfected Foxp3-GFP mice in the presence of 1 μg/ml anti-CD3, 5 μg/ml anti-CD28, 3 ng/ml TGF-β, and 5 ng/ml IL-2. Lungs of 4 mice were pooled for each experiment. The data represent means and SEM of the results of 3 experiments. *, $P < 0.05$; **, $P < 0.01$; #, $P < 0.001$.

Because the CD11b$^+$ CD103$^+$ DCs were augmented in the lungs at day 3 p.i., we examined the blood at days 1 and 2 p.i. for a greater percentage of CD11b$^+$ CD103$^+$ DCs. At day 2 p.i., but not day 1 p.i., the proportion of CD11b$^+$ CD103$^+$ DCs to total CD11c$^+$ CD11b$^+$ MHC-II$^+$ DCs was increased in the circulation of anti-TNF-treated *H. capsulatum*-infected mice compared to control mice (Fig. 5I), indicating the CD11b$^+$ CD103$^+$ DCs migrate through the blood, and in elevated proportions, when TNF is neutralized. CD11b$^+$ CD103$^+$ DCs were present in the lymph nodes at day 3 p.i., but there was no difference between control mice and anti-TNF-treated mice (see Fig. S4 in the supplemental material).

Recently, two markers, CD101 and TREM1, have been shown to define the intestinal CD11b$^+$ CD103$^+$ DC population. CD101 and TREM1 are absent from other cDC subsets in the intestine and both CD103$^+$ and CD11b$^+$ cDCs in the lung (43). To determine the origin of the CD11b$^+$ CD103$^+$ lung DCs, lungs from *H. capsulatum*-infected mice treated with anti-TNF or isotype control antibody were stained for CD101 and TREM1. Consistent with recent findings of intestinal DC CD101 and TREM1 expression, around 75% of CD11b$^+$ CD103$^+$ DCs in the lungs of anti-TNF-treated and control mice displayed CD101 and TREM1 (Fig. 5J), signifying the CD11b$^+$ CD103$^+$ DCs were of gut origin.

DISCUSSION

In this study, we established that the principal cell population responsible for the increased Tregs in TNF-neutralized mice infected with *H. capsulatum* is CD11b$^+$ CD103$^+$ DCs. Total cDC2s from the lungs amplified Tregs *in vitro*, and in the absence of the CD11b$^+$ CD103$^+$ subset, cDC2s failed to expand Tregs. Because this population is understood to be unique to the intestines, we surmised that the cells were migrating from the gut to the lung. The proportion of CD11b$^+$ CD103$^+$ DCs is enhanced in the blood, and they are present in the lymph nodes, and by using fluorescent *H. capsulatum* or beads to label the gut cells, we confirmed the bead-containing CD11b$^+$ CD103$^+$ DCs were present in the lungs. Because the CD11b$^+$ CD103$^+$ DCs are present in equal percentages in the lymph nodes of anti-TNF and isotype control antibody-treated mice, we speculate the intestinal CD11b$^+$ CD103$^+$ DCs migrate from blood to lymph nodes to lung. In the absence of TNF, CD11b$^+$ CD103$^+$ DCs migrate in higher percentages to the lungs from the lymph nodes. To our knowledge, we are the first to report that DCs migrate from the intestinal tract to the lungs.

TNF directly impacts the function of Tregs. Phosphorylation of Foxp3 at Ser418 controls the transcriptional activity and ultimately the suppressive activity of Tregs. TNF signaling produces a protein phosphatase, PP1, that dephosphorylates Foxp3 Ser418, leading to Treg dysfunction (44). It is less clear how Treg function is directly influenced by the absence of TNF. Rheumatoid arthritis patients have a defect in Treg number and function, and those who respond to anti-TNF therapy display rescued Treg function and increased numbers (33). The augmentation of Tregs is recapitulated in mice treated with anti-TNF (4). Although it is possible that the absence of TNF impacts several cell populations, in our model, augmentation of Tregs was not due to direct effects of the absence of TNF on Tregs, but rather, to Treg induction by DCs.

DCs not only promote tolerance, but also aid in *H. capsulatum* clearance. Mice displayed decreased cDC2 numbers starting at day 1 p.i.; however, this reduction was not dependent on *H. capsulatum* infection, as uninfected mice treated with anti-TNF also exhibited a decrement in cDC2s. Diminished DC numbers upon TNF neutralization emerge in other pulmonary fungal infections, including *Cryptococcus neoformans*; however, the loss is not seen until 2 weeks p.i. (45, 46). The abatement in cDC2s beginning at day 1 p.i. likely contributes to impaired immunity to *H. capsulatum*. The decline in DCs is also observed in people receiving anti-TNF therapy. Patients with psoriatic plaques responding to the TNF antagonist etanercept display diminished dermal DCs in plaques, due to either decreased infiltration (47) or apoptosis (48). Anti-TNF treatment also reduces levels of the DC chemoattractant chemerin in sera of rheumatoid arthritis patients (49). Treatment with the anti-TNF therapy adalimumab in

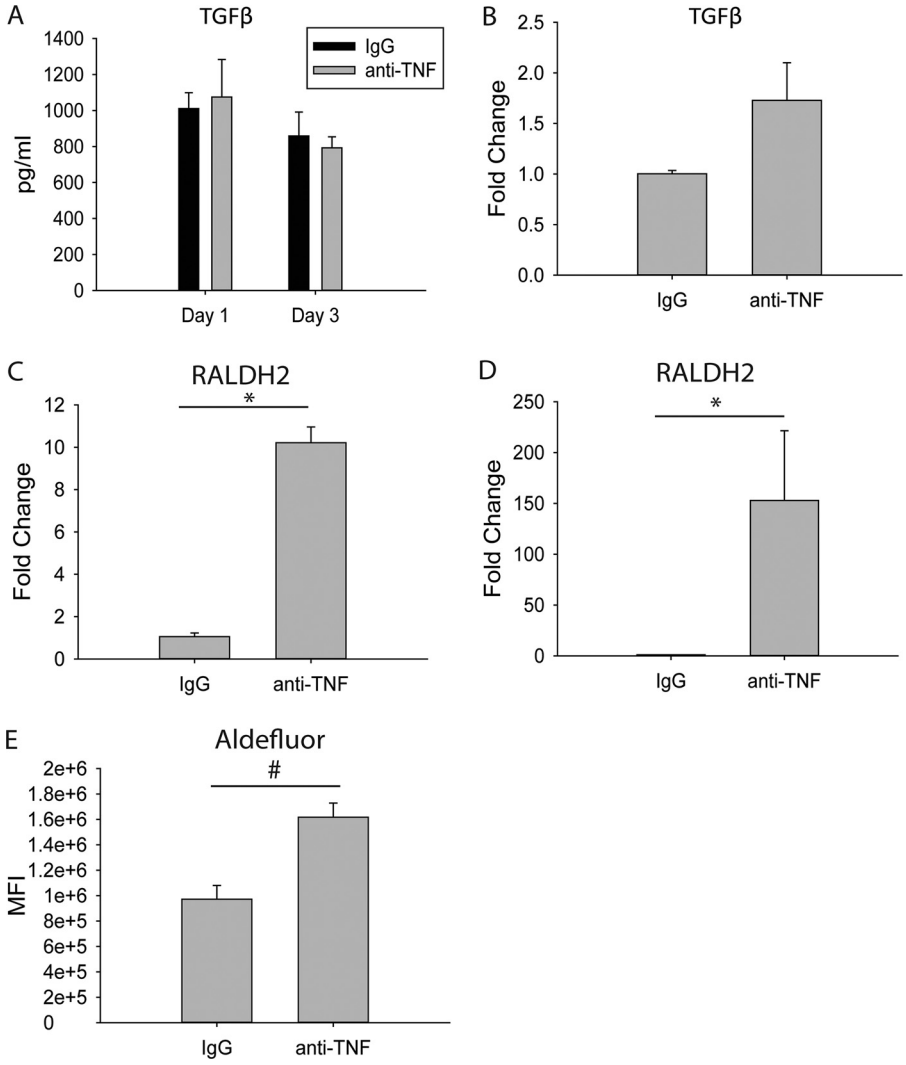

FIG 4 RALDH2 expression and ALDH activity are increased in CD11b$^+$ CD103$^+$ DCs from anti-TNF-treated, *H. capsulatum*-infected mice. Mice were infected with 2×10^6 *H. capsulatum* yeasts i.n. and treated with anti-TNF or isotype control antibody. Lungs were harvested at days 1 and 3 p.i. (A) Protein concentrations were determined in lung homogenates by ELISA. The data represent means and SEM ($n = 8$ mice/group; representative of the results of two experiments) (B) CD11c$^+$ CD11b$^+$ MHC-II$^+$ CD103$^+$ DCs were assessed by FACS from day 3 p.i. lungs, and RNA was extracted. TGF-β gene expression was assessed by qRT-PCR. (C and D) CD11c$^+$ CD11b$^+$ MHC-II$^+$ DCs (C) or CD11c$^+$ CD11b$^+$ MHC-II$^+$ CD103$^+$ DCs (D) were assessed by FACS from lungs, and RNA was extracted. Lungs of 4 mice were pooled for each experiment. The data represent means and SEM of the results of at least 3 experiments. (E) Aldefluor expression was assessed by FACS. The data represent means and SEM ($n = 8$ mice/group; representative of the results of two experiments). *, $P < 0.05$; #, $P < 0.001$.

patients with the inflammatory dermal disease hidradenitis suppurativa results in fewer CD11c$^+$ DCs in inflamed skin (50). The cause of the decrement in DCs with TNF antagonism remains unknown, but it may be related to DC reliance on TNF for maturation (51, 52) and survival (53, 54). *In vitro*, TNF blockade induces DC apoptosis, and the surviving DCs display a semimature phenotype (55). Because the decline in DCs begins at day 1 p.i. and is sustained throughout the course of infection, we speculate that the cause is a combination of factors, including reduced recruitment to the lung and insufficient DC maturity.

The increase in the CD11b$^+$ CD103$^+$ DC population in the lungs is unexpected. CD11b$^+$ CD103$^+$ DCs have been previously described only in the lungs of 129S6/SvEv mice (56). Batf3 knockout mice on this background, which are deficient in CD103$^+$ cDC1s, display reduced percentages and numbers of CD11b$^+$ CD103$^+$ DCs in their

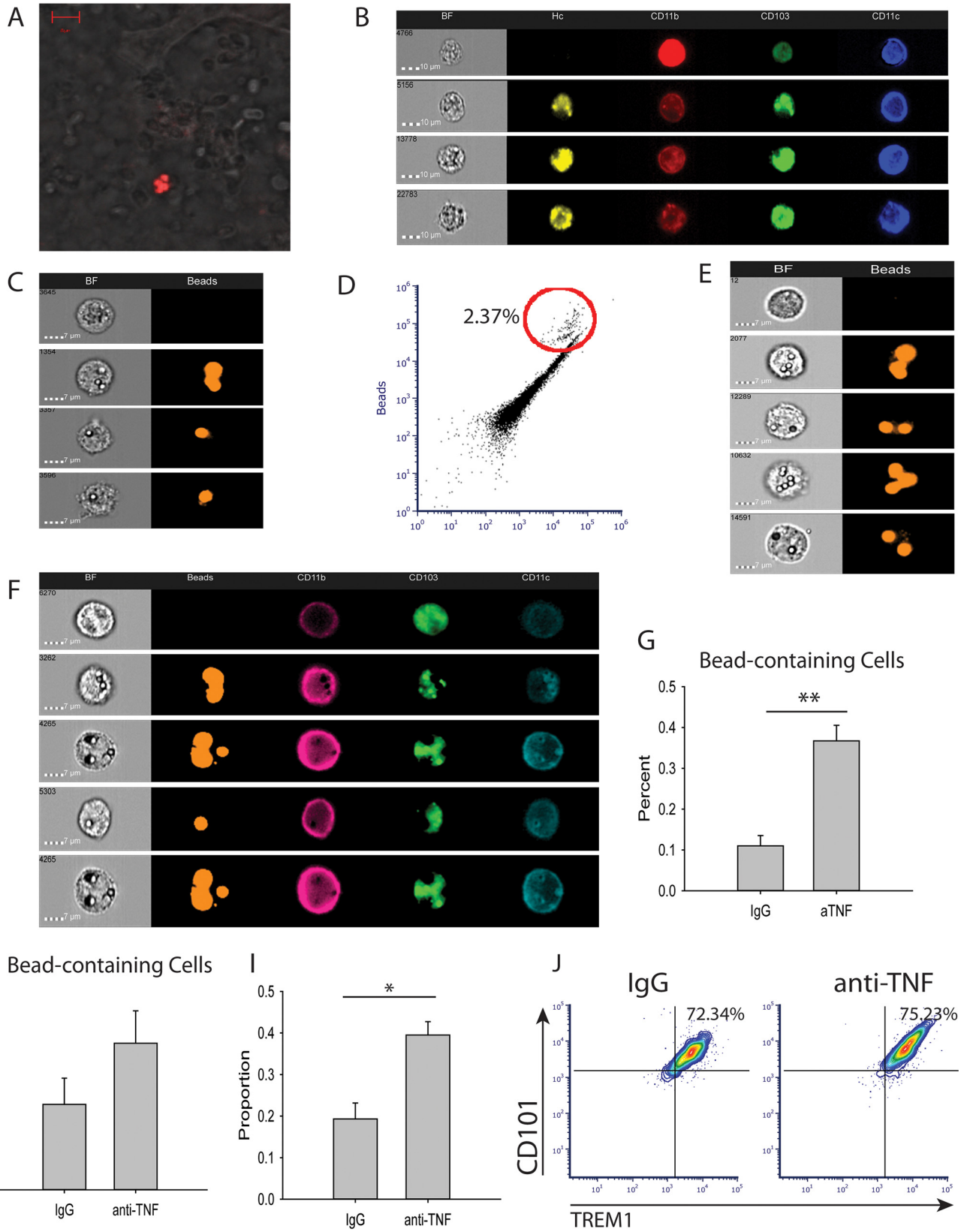

FIG 5 CD11b$^+$ CD103$^+$ DCs migrate from the gut to the lung. Mice were infected with 2×10^6 *H. capsulatum* yeasts i.n. and treated with anti-TNF or isotype control antibody. (A and B) At the time of infection, 4×10^6 tdTomato-*H. capsulatum* yeasts were delivered via oral gavage. Lungs were harvested at day 3 p.i. and assessed by confocal microscopy (A) and Amnis ImagestreamX (B). The data are representative of the results of two experiments containing 8 mice/group. BF, bright field. (C and D) Mice were treated with 4×10^6 beads i.n., and lungs were harvested 3 days after treatment. Bead-containing cells were

(Continued on next page)

lungs compared to control mice (56), suggesting lung CD11b$^+$ CD103$^+$ DCs belong to the cDC1 group. Contrary to these findings, it has been speculated that in the lungs, the CD103$^-$ cDC2s upregulate CD103 under inflammatory conditions to produce a CD11b$^+$ CD103$^+$ population; however, no published data exist to support this conclusion (57).

The increase in CD11b$^+$ CD103$^+$ DCs is specific to TNF neutralization, as it does not develop in *H. capsulatum*-infected mice administered neutralizing antibody to IFN-γ. Patients with inflammatory bowel disease (IBD) exhibit reduced numbers of CD103$^+$ DCs in the inflamed intestine, and treatment with the TNF antagonist adalimumab reverses this decrement (58, 59). The cause of the diminished CD103$^+$ DCs transpiring during IBD is unknown; however, it has been speculated that it is attributable to changes in migration (60). This would be consistent with our findings, as the CD11b$^+$ CD103$^+$ DCs migrate from the gut to the lung in mice infected with *H. capsulatum* and treated with anti-TNF. The fraction of DCs that express ALDH is also diminished in ulcerative colitis patients, suggesting retinoic acid influences intestinal health and suppression of inflammation.

Retinoic acid secretion by CD103$^+$ DCs induces Tregs by enhancing TGF-β signaling and suppressing the action of interleukin 6 (IL-6) (27, 28, 61). Lamina propria CD11b$^+$ CD103$^+$ DCs in mice and CD103$^+$ DCs in humans have been shown to express RALDH2 (27, 62, 63). Retinoic acid-secreting CD11b$^+$ CD103$^+$ DCs shape Tregs, not only in the gastrointestinal (GI) tract, but also in the skin during development. In neonatal mice, commensal fungi drive intestinal CD11b$^+$ CD103$^+$ RALDH$^+$ DC migration to gut-draining mesenteric lymph nodes. Surprisingly, the CD11b$^+$ CD103$^+$ RALDH$^+$ DCs also migrate to the skin-draining inguinal lymph nodes via the efferent lymph and bloodstream. However, the trafficking of these cells to the inguinal lymph nodes is restricted to the first 4 weeks of life (63), contrary to our findings of migration of CD11b$^+$ CD103$^+$ DCs in adult mice.

Interaction along the gut/lung axis is not a new phenomenon. Up to 50% of adult patients with IBD present with lung involvement, including lung inflammation or impaired lung function (64–67). The gut microbiota affects immunity at distal sites, including the lung. Allergic asthma is ameliorated by gastric *Helicobacter pylori* extract treatment; improvement in asthma symptoms is dependent on enrichment of *Batf3*-dependent CD11b$^-$ CD103$^+$ DCs in the lungs (68). Under certain conditions, including a murine sepsis model, the gut microbiota can migrate to the lungs (69), demonstrating a direct migration along the gut/lung axis. However, the translocation of CD11b$^+$ CD103$^+$ DCs had not been observed prior to our studies. We show relocation of resident cDCs to the lungs during pulmonary *H. capsulatum* infection (Fig. 5F and J) and that anti-TNF treatment results in dysregulated coordination between the gut and lung with regard to CD11b$^+$ CD103$^+$ DCs (Fig. 5G). Treatment with TNF antagonism leads to susceptibility to other pulmonary infections, including the fungal pathogens *Aspergillus fumigatus*, *Blastomyces*, and *Coccidioides* and the intracellular bacterium *Mycobacterium tuberculosis*. Whether the CD11b$^+$ CD103$^+$ DCs migrate from the gut to the lung and ultimately reduce clearance of the other pathogens by amplifying Treg numbers remains unresolved.

In summary, we identified the vital subset of DCs responsible for Treg amplification in TNF-neutralized, *H. capsulatum*-infected mice. It is commonly accepted that the CD11b$^+$ CD103$^+$ DCs are exclusive to the intestinal tract; however, we show compelling evidence that the CD11b$^+$ CD103$^+$ DCs migrate from the gut to the lung under these inflammatory conditions. The CD11b$^+$ CD103$^+$ DCs express RALDH2 and manifest increased activity of RALDH. Preventing the migration of the CD11b$^+$ CD103$^+$ DCs

FIG 5 Legend (Continued)
assessed by Amnis ImagestreamX. The data are representative of two mice. (E to H) Mice were treated with 4×10^7 beads via oral gavage on days 0, 1, and 2 p.i. Lungs were harvested at day 3 p.i. and assessed by Amnis ImagestreamX. (I) Blood was drawn from the mice at day 2 p.i., and DCs were assessed by FACS. (J) Lungs were harvested at day 3 p.i., and DCs were assessed by FACS. The data represent means and SEM ($n = 8$ mice/group; representative of the results of two experiments). *, $P < 0.05$; **, $P < 0.01$.

could potentially be used to prevent susceptibility to infections when TNF is neutralized.

MATERIALS AND METHODS

Mice. C57BL/6 (wild-type [WT]) and Foxp3-GFP mice were obtained from Jackson Laboratory and maintained by the Department of Laboratory Animal Medicine, University of Cincinnati, which is accredited by the American Association for Accreditation of Laboratory Animal Medicine. Animal experiments were in accordance with the Animal Welfare Act guidelines of the National Institutes of Health.

Preparation of *H. capsulatum* and infection of mice. The *H. capsulatum* yeast strains G217B and tdTomato-expressing G217B (kindly provided by Chad Rappleye, Ohio State University) were grown for 72 h at 37°C as previously described (3). To produce infection in mice, 6- to 12-week-old mice were inoculated i.n. with 2×10^6 yeast cells in an approximately 30 μl of Hanks' balanced salt solution (HBSS) (HyClone, Logan, UT).

***In vivo* neutralization of TNF-α.** At the time of infection, mice were given an intraperitoneal (i.p.) injection of 1 mg/0.5 ml rat anti-mouse TNF-α from cell line XT-22.1 (National Cell Culture Center, Minneapolis, MN).

Isolation of lung leukocytes. Lungs were homogenized in 5 ml of HBSS using a gentleMACS Dissociator (Miltenyi Biotec) and incubated with 40 U of DNase I (Roche, Mannheim, Germany) and 2 mg/ml of collagenase D (Roche) for 30 min at 37°C. The dissociated lungs were filtered through a 40-μm nylon mesh (Spectrum Laboratories, Rancho Dominguez, CA). Leukocytes were isolated using Lympholyte M (Cedarlane Laboratories, Burlington, ON, Canada). All cell solutions were filtered through 60-μm nylon mesh (Spectrum Laboratories).

Flow cytometry and cell sorting. Cells were washed with 1% bovine serum albumin in HBSS (pH 7.4) and stained at 4°C for 30 min. The cells were analyzed using the BD Accuri C6 (BD Biosciences, San Jose, CA) and FCS Express software or Amnis ImagestreamX and analyzed with Amnis Ideas software. The cells were sorted on a MoFlo XDP (Beckman Coulter, Brea, CA). The following monoclonal antibodies (MAbs) were purchased from BD Biosciences: IAb-fluorescein isothiocyanate (FITC), CD103$^-$ phycoerythrin (PE), CD11b$^-$ peridinin chlorophyll protein (PerCP), CD11c$^-$ allophycocyanin (APC), CD11b$^-$ APC-Cy7, CD103$^-$ BV510, CD11c$^-$ PE-Cy7, CD25$^-$ APC, CD4$^-$ PE, CD3$^-$ PerCP, and CD274 (PD-L1)-PE. The following MAbs were purchased from eBioscience: TREM1-eFluor660, CD101$^-$ PE-Cy7, and CD11c$^-$ APCeFluor780. F4/80-APC and CD273 (PD-L2)-APC were purchased from BioLegend. The gating strategy for isolation of CD11b$^+$ CD103$^+$ DCs can be found in Fig. S2 in the supplemental material.

Assessment of ALDH activity. ALDH activity was assessed using the Aldefluor kit (StemCell, Vancouver, Canada). Cells were stained according to the manufacturer's instructions. For each sample, 1×10^6 cells were suspended in 1 ml Aldefluor assay buffer with 5 μl activated Aldefluor reagent in the presence or absence of the ALDH inhibitor diethylaminobenzaldehyde. Samples were incubated at 37°C for 45 min.

DC/alveolar macrophage and T cell coculture. DCs or alveolar macrophages were assessed by FACS from mouse lungs and cocultured with FACS-assessed splenic CD4$^+$ CD25$^-$ Foxp3$^-$ T cells from uninfected Foxp3-GFP mice in a ratio of 1 DC or alveolar macrophage to 10 T cells for 5 days in the presence of 1 μg/ml anti-CD3, 5 μg/ml anti-CD28, 3 ng/ml TGF-β, and 5 ng/ml IL-2 (Peprotech, Rocky Hill, NJ).

RNA isolation, cDNA synthesis, and qRT-PCR. RNA was isolated from whole lungs of mice using TRIzol (Invitrogen), and RNA was isolated from FACS-assessed DCs and T cells using an RNAeasy kit (Qiagen, Valencia, CA). Oligo(dT)-primed cDNA was prepared using the reverse transcriptase system (Promega, Madison WI). Quantitative reverse transcription-PCR (qRT-PCR) analysis was performed using TaqMan master mixture and primers obtained from Applied Biosystems (Foster City, CA). Samples were analyzed with an ABI Prism 7500. The beta-2 microglobulin gene was used as an internal control. The conditions for amplification were 50°C for 2 min and 95°C for 10 min, followed by 40 cycles of 95°C for 15s and 60°C for 1 min.

Cytokine and chemokine quantification. Mouse TGF-β1 enzyme-linked immunosorbent assay (ELISA) material was purchased from R&D Systems.

Oral gavage of *H. capsulatum* or beads. Four million tdTomato-*H. capsulatum* yeasts suspended in 100 μl HBSS were orally gavaged concurrently with anti-TNF treatment and i.n. infection. Forty million purple carboxyl fluorescent particles (1.7 to 2.2 μm; catalog number CFP-2062-2; Spherotech, Lake Forest, IL) were suspended in 100 μl sterile water and orally gavaged daily for 3 days.

Confocal microscopic analysis of lung tissue. Lungs were fixed with 10% formalin, removed, and embedded in paraffin blocks. Sections were viewed on a Zeiss LSM 510 confocal microscope and analyzed using Zeiss Zen software.

Statistics. Nonpaired Student *t* tests were used for two-group comparisons.

SUPPLEMENTAL MATERIAL

Supplemental material for this article may be found at https://doi.org/10.1128/IAI.00109-18.

SUPPLEMENTAL FILE 1, PDF file, 0.4 MB.

ACKNOWLEDGMENTS

We thank William Buesing for technical assistance.

This work was supported by Merit Award I01BX000717 from the Veterans Affairs Department and by NIH grants AI-106269 and AI-126818.

G.S.D. and J.L.T. designed experiments, conceptualized questions, and wrote the manuscript. J.L.T. performed experiments and analyzed data.

REFERENCES

1. Tsiodras S, Samonis G, Boumpas DT, Kontoyiannis DP. 2008. Fungal infections complicating tumor necrosis factor alpha blockade therapy. Mayo Clin Proc 83:181–194.
2. Wood KL, Hage CA, Knox KS, Kleiman MB, Sannuti A, Day RB, Wheat LJ, Twigg HL. 2003. Histoplasmosis after treatment with anti-tumor necrosis factor-alpha therapy. Am J Respir Crit Care Med 167:1279–1282. https://doi.org/10.1164/rccm.200206-563OC.
3. Allendoerfer R, Deepe GS. 1998. Blockade of endogenous TNF-alpha exacerbates primary and secondary pulmonary histoplasmosis by differential mechanisms. J Immunol 160:6072–6082.
4. Deepe GS, Gibbons RS. 2008. TNF-alpha antagonism generates a population of antigen-specific CD4+CD25+ T cells that inhibit protective immunity in murine histoplasmosis. J Immunol 180:1088–1097. https://doi.org/10.4049/jimmunol.180.2.1088.
5. Kroetz DN, Deepe GS, Jr. 2012. CCR5 deficiency mitigates the deleterious effects of tumor necrosis factor α antagonism in murine histoplasmosis. J Infect Dis 205:955–963. https://doi.org/10.1093/infdis/jir869.
6. Guilliams M, Ginhoux F, Jakubzick C, Naik SH, Onai N, Schraml BU, Segura E, Tussiwand R, Yona S. 2014. Dendritic cells, monocytes and macrophages: a unified nomenclature based on ontogeny. Nat Rev Immunol 14:571–578. https://doi.org/10.1038/nri3712.
7. Guilliams M, Dutertre C-A, Scott CL, McGovern N, Sichien D, Chakarov S, Van Gassen S, Chen J, Poidinger M, De Prijck S, Tavernier SJ, Low I, Irac SE, Mattar CN, Sumatoh HR, Low GHL, Chung TJK, Chan DKH, Tan KK, Hon TLK, Fossum E, Bogen B, Choolani M, Chan JKY, Larbi A, Luche H, Henri S, Saeys Y, Newell EW, Lambrecht BN, Malissen B, Ginhoux F. 2016. Unsupervised high-dimensional analysis aligns dendritic cells across tissues and species. Immunity 45:669–684. https://doi.org/10.1016/j.immuni.2016.08.015.
8. Hildner K, Edelson BT, Purtha WE, Diamond M, Matsushita H, Kohyama M, Calderon B, Schraml BU, Unanue ER, Diamond MS, Schreiber RD, Murphy TL, Murphy KM. 2008. Batf3 deficiency reveals a critical role for CD8alpha+ dendritic cells in cytotoxic T cell immunity. Science 322:1097–1100. https://doi.org/10.1126/science.1164206.
9. Grajales-Reyes GE, Iwata A, Albring J, Wu X, Tussiwand R, Kc W, Kretzer NM, Briseño CG, Durai V, Bagadia P, Haldar M, Schönheit J, Rosenbauer F, Murphy TL, Murphy KM. 2015. Batf3 maintains autoactivation of Irf8 for commitment of a CD8α(+) conventional DC clonogenic progenitor. Nat Immunol 16:708–717. https://doi.org/10.1038/ni.3197.
10. Sichien D, Scott CL, Martens L, Vanderkerken M, Van Gassen S, Plantinga M, Joeris T, De Prijck S, Vanhoutte L, Vanheerswynghels M, Van Isterdael G, Toussaint W, Madeira FB, Vergote K, Agace WW, Clausen BE, Hammad H, Dalod M, Saeys Y, Lambrecht BN, Guilliams M. 2016. IRF8 transcription factor controls survival and function of terminally differentiated conventional and plasmacytoid dendritic cells, respectively. Immunity 45:626–640. https://doi.org/10.1016/j.immuni.2016.08.013.
11. Ginhoux F, Liu K, Helft J, Bogunovic M, Greter M, Hashimoto D, Price J, Yin N, Bromberg J, Lira SA, Stanley ER, Nussenzweig M, Merad M. 2009. The origin and development of nonlymphoid tissue CD103+ DCs. J Exp Med 206:3115–3130. https://doi.org/10.1084/jem.20091756.
12. Crozat K, Tamoutounour S, Vu Manh T-P, Fossum E, Luche H, Ardouin L, Guilliams M, Azukizawa H, Bogen B, Malissen B, Henri S, Dalod M. 2011. Cutting edge: expression of XCR1 defines mouse lymphoid-tissue resident and migratory dendritic cells of the CD8α+ type. J Immunol 187:4411–4415. https://doi.org/10.4049/jimmunol.1101717.
13. Bachem A, Hartung E, Güttler S, Mora A, Zhou X, Hegemann A, Plantinga M, Mazzini E, Stoitzner P, Gurka S, Henn V, Mages HW, Kroczek RA. 2012. Expression of XCR1 characterizes the Batf3-dependent lineage of dendritic cells capable of antigen cross-presentation. Front Immunol 3:214. https://doi.org/10.3389/fimmu.2012.00214.
14. Cerovic V, Houston SA, Westlund J, Utriainen L, Davison ES, Scott CL, Bain CC, Joeris T, Agace WW, Kroczek RA, Mowat AM, Yrlid U, Milling SWF. 2015. Lymph-borne CD8α+ dendritic cells are uniquely able to cross-prime CD8+ T cells with antigen acquired from intestinal epithelial cells. Mucosal Immunol 8:38–48. https://doi.org/10.1038/mi.2014.40.
15. Schlitzer A, McGovern N, Teo P, Zelante T, Atarashi K, Low D, Ho AWS, See P, Shin A, Wasan PS, Hoeffel G, Malleret B, Heiseke A, Chew S, Jardine L, Purvis HA, Hilkens CMU, Tam J, Poidinger M, Stanley ER, Krug AB, Renia L, Sivasankar B, Ng LG, Collin M, Ricciardi-Castagnoli P, Honda K, Haniffa M, Ginhoux F. 2013. IRF4 transcription factor-dependent CD11b+ dendritic cells in human and mouse control mucosal IL-17 cytokine responses. Immunity 38:970–983. https://doi.org/10.1016/j.immuni.2013.04.011.
16. Persson EK, Uronen-Hansson H, Semmrich M, Rivollier A, Hägerbrand K, Marsal J, Gudjonsson S, Håkansson U, Reizis B, Kotarsky K, Agace WW. 2013. IRF4 transcription-factor-dependent CD103(+)CD11b(+) dendritic cells drive mucosal T helper 17 cell differentiation. Immunity 38:958–969. https://doi.org/10.1016/j.immuni.2013.03.009.
17. Bajaña S, Turner S, Paul J, Ainsua-Enrich E, Kovats S. 2016. IRF4 and IRF8 act in CD11c+ cells to regulate terminal differentiation of lung tissue dendritic cells. J Immunol 196:1666–1677. https://doi.org/10.4049/jimmunol.1501870.
18. Dudziak D, Kamphorst AO, Heidkamp GF, Buchholz VR, Trumpfheller C, Yamazaki S, Cheong C, Liu K, Lee H-W, Park CG, Steinman RM, Nussenzweig MC. 2007. Differential antigen processing by dendritic cell subsets in vivo. Science 315:107–111. https://doi.org/10.1126/science.1136080.
19. Idoyaga J, Cheong C, Suda K, Suda N, Kim JY, Lee H, Park CG, Steinman RM. 2008. Cutting edge: langerin/CD207 receptor on dendritic cells mediates efficient antigen presentation on MHC I and II products in vivo. J Immunol 180:3647–3650. https://doi.org/10.4049/jimmunol.180.6.3647.
20. Bedoui S, Whitney PG, Waithman J, Eidsmo L, Wakim L, Caminschi I, Allan RS, Wojtasiak M, Shortman K, Carbone FR, Brooks AG, Heath WR. 2009. Cross-presentation of viral and self antigens by skin-derived CD103+ dendritic cells. Nat Immunol 10:488–495. https://doi.org/10.1038/ni.1724.
21. Kim TS, Braciale TJ. 2009. Respiratory dendritic cell subsets differ in their capacity to support the induction of virus-specific cytotoxic CD8+ T cell responses. PLoS One 4:e4204. https://doi.org/10.1371/journal.pone.0004204.
22. Kastenmüller K, Wille-Reece U, Lindsay RWB, Trager LR, Darrah PA, Flynn BJ, Becker MR, Udey MC, Clausen BE, Igyarto BZ, Kaplan DH, Kastenmüller W, Germain RN, Seder RA. 2011. Protective T cell immunity in mice following protein-TLR7/8 agonist-conjugate immunization requires aggregation, type I IFN, and multiple DC subsets. J Clin Invest 121:1782–1796. https://doi.org/10.1172/JCI45416.
23. McLachlan JB, Catron DM, Moon JJ, Jenkins MK. 2009. Dendritic cell antigen presentation drives simultaneous cytokine production by effector and regulatory T cells in inflamed skin. Immunity 30:277–288. https://doi.org/10.1016/j.immuni.2008.11.013.
24. Guilliams M, Crozat K, Henri S, Tamoutounour S, Grenot P, Devilard E, de Bovis B, Alexopoulou L, Dalod M, Malissen B. 2010. Skin-draining lymph nodes contain dermis-derived CD103(−) dendritic cells that constitutively produce retinoic acid and induce Foxp3(+) regulatory T cells. Blood 115:1958–1968. https://doi.org/10.1182/blood-2009-09-245274.
25. Vitali C, Mingozzi F, Broggi A, Barresi S, Zolezzi F, Bayry J, Raimondi G, Zanoni I, Granucci F. 2012. Migratory, and not lymphoid-resident, dendritic cells maintain peripheral self-tolerance and prevent autoimmunity via induction of iTreg cells. Blood 120:1237–1245. https://doi.org/10.1182/blood-2011-09-379776.
26. Lewis KL, Caton ML, Bogunovic M, Greter M, Grajkowska LT, Ng D, Klinakis A, Charo IF, Jung S, Gommerman JL, Ivanov II, Liu K, Merad M, Reizis B. 2011. Notch2 receptor signaling controls functional differenti-

ation of dendritic cells in the spleen and intestine. Immunity 35: 780–791. https://doi.org/10.1016/j.immuni.2011.08.013.
27. Coombes JL, Siddiqui KRR, Arancibia-Cárcamo CV, Hall J, Sun C-M, Belkaid Y, Powrie F. 2007. A functionally specialized population of mucosal CD103+ DCs induces Foxp3+ regulatory T cells via a TGF-beta and retinoic acid-dependent mechanism. J Exp Med 204:1757–1764. https://doi.org/10.1084/jem.20070590.
28. Sun C-M, Hall JA, Blank RB, Bouladoux N, Oukka M, Mora JR, Belkaid Y. 2007. Small intestine lamina propria dendritic cells promote de novo generation of Foxp3 T reg cells via retinoic acid. J Exp Med 204: 1775–1785. https://doi.org/10.1084/jem.20070602.
29. Fontenot JD, Gavin MA, Rudensky AY. 2003. Foxp3 programs the development and function of CD4+CD25+ regulatory T cells. Nat Immunol 4:330–336. https://doi.org/10.1038/ni904.
30. Khattri R, Cox T, Yasayko S-A, Ramsdell F. 2003. An essential role for Scurfin in CD4+CD25+ T regulatory cells. Nat Immunol 4:337–342.
31. Hori S, Nomura T, Sakaguchi S. 2003. Control of regulatory T cell development by the transcription factor Foxp3. Science 299:1057–1061. https://doi.org/10.1126/science.1079490.
32. Floess S, Freyer J, Siewert C, Baron U, Olek S, Polansky J, Schlawe K, Chang H-D, Bopp T, Schmitt E, Klein-Hessling S, Serfling E, Hamann A, Huehn J. 2007. Epigenetic control of the foxp3 locus in regulatory T cells. PLoS Biol 5:e38. https://doi.org/10.1371/journal.pbio.0050038.
33. Ehrenstein MR, Evans JG, Singh A, Moore S, Warnes G, Isenberg DA, Mauri C. 2004. Compromised function of regulatory T cells in rheumatoid arthritis and reversal by anti-TNFalpha therapy. J Exp Med 200: 277–285. https://doi.org/10.1084/jem.20040165.
34. Thornton AM, Korty PE, Tran DQ, Wohlfert EA, Murray PE, Belkaid Y, Shevach EM. 2010. Expression of Helios, an Ikaros transcription factor family member, differentiates thymic-derived from peripherally induced Foxp3+ T regulatory cells. J Immunol 184:3433–3441. https://doi.org/10.4049/jimmunol.0904028.
35. Khare A, Krishnamoorthy N, Oriss TB, Fei M, Ray P, Ray A. 2013. Cutting edge: inhaled antigen upregulates retinaldehyde dehydrogenase in lung CD103+ but not plasmacytoid dendritic cells to induce Foxp3 de novo in CD4+ T cells and promote airway tolerance. J Immunol 191:25–29. https://doi.org/10.4049/jimmunol.1300193.
36. Coleman MM, Ruane D, Moran B, Dunne PJ, Keane J, Mills KHG. 2013. Alveolar macrophages contribute to respiratory tolerance by inducing FoxP3 expression in naive T cells. Am J Respir Cell Mol Biol 48:773–780. https://doi.org/10.1165/rcmb.2012-0263OC.
37. Soroosh P, Doherty TA, Duan W, Mehta AK, Choi H, Adams YF, Mikulski Z, Khorram N, Rosenthal P, Broide DH, Croft M. 2013. Lung-resident tissue macrophages generate Foxp3+ regulatory T cells and promote airway tolerance. J Exp Med 210:775–788. https://doi.org/10.1084/jem.20121849.
38. Denning TL, Norris BA, Medina-Contreras O, Manicassamy S, Geem D, Madan R, Karp CL, Pulendran B. 2011. Functional specializations of intestinal dendritic cell and macrophage subsets that control Th17 and regulatory T cell responses are dependent on the T Cell/APC ratio, source of mouse strain, and regional localization. J Immunol 187: 733–747. https://doi.org/10.4049/jimmunol.1002701.
39. Francisco LM, Salinas VH, Brown KE, Vanguri VK, Freeman GJ, Kuchroo VK, Sharpe AH. 2009. PD-L1 regulates the development, maintenance, and function of induced regulatory T cells. J Exp Med 206:3015–3029. https://doi.org/10.1084/jem.20090847.
40. DiPaolo RJ, Brinster C, Davidson TS, Andersson J, Glass D, Shevach EM. 2007. Autoantigen-specific TGFbeta-induced Foxp3+ regulatory T cells prevent autoimmunity by inhibiting dendritic cells from activating autoreactive T cells. J Immunol 179:4685–4693. https://doi.org/10.4049/jimmunol.179.7.4685.
41. Allendoerfer R, Deepe GS. 1997. Intrapulmonary response to Histoplasma capsulatum in gamma interferon knockout mice. Infect Immun 65:2564–2569.
42. Hill JA, Hall JA, Sun C-M, Cai Q, Ghyselinck N, Chambon P, Belkaid Y, Mathis D, Benoist C. 2008. Retinoic acid enhances Foxp3 induction indirectly by relieving inhibition from CD4+CD44hi Cells. Immunity 29:758–770. https://doi.org/10.1016/j.immuni.2008.09.018.
43. Bain CC, Montgomery J, Scott CL, Kel JM, Girard-Madoux MJH, Martens L, Zangerle-Murray TFP, Ober-Blöbaum J, Lindenbergh-Kortleve D, Samsom JN, Henri S, Lawrence T, Saeys Y, Malissen B, Dalod M, Clausen BE, Mowat AM. 2017. TGFβR signalling controls CD103(+)CD11b(+) dendritic cell development in the intestine. Nat Commun 8:620. https://doi.org/10.1038/s41467-017-00658-6.
44. Nie H, Zheng Y, Li R, Guo TB, He D, Fang L, Liu X, Xiao L, Chen X, Wan B, Chin YE, Zhang JZ. 2013. Phosphorylation of FOXP3 controls regulatory T cell function and is inhibited by TNF-α in rheumatoid arthritis. Nat Med 19:322–328. https://doi.org/10.1038/nm.3085.
45. Herring AC, Falkowski NR, Chen G-H, McDonald RA, Toews GB, Huffnagle GB. 2005. Transient neutralization of tumor necrosis factor alpha can produce a chronic fungal infection in an immunocompetent host: potential role of immature dendritic cells. Infect Immun 73:39–49. https://doi.org/10.1128/IAI.73.1.39-49.2005.
46. Xu J, Eastman AJ, Flaczyk A, Neal LM, Zhao G, Carolan J, Malachowski AN, Stolberg VR, Yosri M, Chensue SW, Curtis JL, Osterholzer JJ, Olszewski MA. 2016. Disruption of early tumor necrosis factor alpha signaling prevents classical activation of dendritic cells in lung-associated lymph nodes and development of protective immunity against cryptococcal infection. mBio 7:e00510-16. https://doi.org/10.1128/mBio.00510-16.
47. Gottlieb AB, Chamian F, Masud S, Cardinale I, Abello MV, Lowes MA, Chen F, Magliocco M, Krueger JG. 2005. TNF inhibition rapidly downregulates multiple proinflammatory pathways in psoriasis plaques. J Immunol 175:2721–2729. https://doi.org/10.4049/jimmunol.175.4.2721.
48. Malaviya R, Sun Y, Tan JK, Wang A, Magliocco M, Yao M, Krueger JG, Gottlieb AB. 2006. Etanercept induces apoptosis of dermal dendritic cells in psoriatic plaques of responding patients. J Am Acad Dermatol 55: 590–597. https://doi.org/10.1016/j.jaad.2006.05.004.
49. Herenius MMJ, Oliveira ASF, Wijbrandts CA, Gerlag DM, Tak PP, Lebre MC. 2013. Anti-TNF therapy reduces serum levels of chemerin in rheumatoid arthritis: a new mechanism by which anti-TNF might reduce inflammation. PLoS One 8:e57802. https://doi.org/10.1371/journal.pone.0057802.
50. van der Zee HH, Laman JD, de Ruiter L, Dik WA, Prens EP. 2012. Adalimumab (antitumour necrosis factor-α) treatment of hidradenitis suppurativa ameliorates skin inflammation: an in situ and ex vivo study. Br J Dermatol 166:298–305. https://doi.org/10.1111/j.1365-2133.2011.10698.x.
51. Sallusto F, Lanzavecchia A. 1994. Efficient presentation of soluble antigen by cultured human dendritic cells is maintained by granulocyte/macrophage colony-stimulating factor plus interleukin 4 and downregulated by tumor necrosis factor alpha. J Exp Med 179:1109–1118. https://doi.org/10.1084/jem.179.4.1109.
52. Miwa S, Nishida H, Tanzawa Y, Takata M, Takeuchi A, Yamamoto N, Shirai T, Hayashi K, Kimura H, Igarashi K, Mizukoshi E, Nakamoto Y, Kaneko S, Tsuchiya H. 2012. TNF-α and tumor lysate promote the maturation of dendritic cells for immunotherapy for advanced malignant bone and soft tissue tumors. PLoS One 7:e52926. https://doi.org/10.1371/journal.pone.0052926.
53. Ludewig B, Graf D, Gelderblom HR, Becker Y, Kroczek RA, Pauli G. 1995. Spontaneous apoptosis of dendritic cells is efficiently inhibited by TRAP (CD40-ligand) and TNF-alpha, but strongly enhanced by interleukin-10. Eur J Immunol 25:1943–1950. https://doi.org/10.1002/eji.1830250722.
54. Pirtskhalaishvili G, Shurin GV, Esche C, Trump DL, Shurin MR. 2001. TNF-alpha protects dendritic cells from prostate cancer-induced apoptosis. Prostate Cancer Prostatic Dis 4:221–227. https://doi.org/10.1038/sj.pcan.4500525.
55. Baldwin HM, Ito-Ihara T, Isaacs JD, Hilkens CMU. 2010. Tumour necrosis factor alpha blockade impairs dendritic cell survival and function in rheumatoid arthritis. Ann Rheum Dis 69:1200–1207. https://doi.org/10.1136/ard.2009.110502.
56. Edelson BT, Juang KCWR, Kohyama M, Benoit LA, Klekotka PA, Moon C, Albring JC, Ise W, Michael DG, Bhattacharya D, Stappenbeck TS, Holtzman MJ, Sung S-SJ, Murphy TL, Hildner K, Murphy KM. 2010. Peripheral CD103+ dendritic cells form a unified subset developmentally related to CD8α+ conventional dendritic cells. J Exp Med 207:823–836. https://doi.org/10.1084/jem.20091627.
57. Guilliams M, Lambrecht BN, Hammad H. 2013. Division of labor between lung dendritic cells and macrophages in the defense against pulmonary infections. Mucosal Immunol 6:464–473. https://doi.org/10.1038/mi.2013.14.
58. Magnusson MK, Brynjólfsson SF, Dige A, Uronen-Hansson H, Börjesson LG, Bengtsson JL, Gudjonsson S, Öhman L, Agnholt J, Sjövall H, Agace WW, Wick MJ. 2016. Macrophage and dendritic cell subsets in IBD: ALDH+ cells are reduced in colon tissue of patients with ulcerative colitis regardless of inflammation. Mucosal Immunol 9:171–182. https://doi.org/10.1038/mi.2015.48.
59. Dige A, Magnusson MK, Öhman L, Hvas CL, Kelsen J, Wick MJ, Agnholt J. 2016. Reduced numbers of mucosal DR(int) macrophages and increased numbers of CD103(+) dendritic cells during anti-TNF-α treat-

ment in patients with Crohn's disease. Scand J Gastroenterol 51:692–699. https://doi.org/10.3109/00365521.2015.1134649.
60. Hinderer S, Shena N, Ringuette L-J, Hansmann J, Reinhardt DP, Brucker SY, Davis EC, Schenke-Layland K. 2015. In vitro elastogenesis: instructing human vascular smooth muscle cells to generate an elastic fiber-containing extracellular matrix scaffold. Biomed Mater 10:034102. https://doi.org/10.1088/1748-6041/10/3/034102.
61. Mucida D, Park Y, Kim G, Turovskaya O, Scott I, Kronenberg M, Cheroutre H. 2007. Reciprocal TH17 and regulatory T cell differentiation mediated by retinoic acid. Science 317:256–260. https://doi.org/10.1126/science.1145697.
62. Iwata M, Hirakiyama A, Eshima Y, Kagechika H, Kato C, Song S-Y. 2004. Retinoic acid imprints gut-homing specificity on T cells. Immunity 21:527–538. https://doi.org/10.1016/j.immuni.2004.08.011.
63. Zhang Z, Li J, Zheng W, Zhao G, Zhang H, Wang X, Guo Y, Qin C, Shi Y. 2016. Peripheral lymphoid volume expansion and maintenance are controlled by gut microbiota via RALDH+ dendritic cells. Immunity 44:330–342. https://doi.org/10.1016/j.immuni.2016.01.004.
64. Yazar A, Atis S, Konca K, Pata C, Akbay E, Calikoglu M, Hafta A. 2001. Respiratory symptoms and pulmonary functional changes in patients with irritable bowel syndrome. Am J Gastroenterol 96:1511–1516. https://doi.org/10.1111/j.1572-0241.2001.03748.x.
65. Ceyhan BB, Karakurt S, Cevik H, Sungur M. 2003. Bronchial hyperreactivity and allergic status in inflammatory bowel disease. Respiration 70:60–66. https://doi.org/10.1159/000068407.
66. Douglas JG, McDonald CF, Leslie MJ, Gillon J, Crompton GK, McHardy GJ. 1989. Respiratory impairment in inflammatory bowel disease: does it vary with disease activity? Respir Med 83:389–394. https://doi.org/10.1016/S0954-6111(89)80070-8.
67. Songür N, Songür Y, Tüzün M, Doğan I, Tüzün D, Ensari A, Hekimoglu B. 2003. Pulmonary function tests and high-resolution CT in the detection of pulmonary involvement in inflammatory bowel disease. J Clin Gastroenterol 37:292–298. https://doi.org/10.1097/00004836-200310000-00006.
68. Engler DB, Reuter S, van Wijck Y, Urban S, Kyburz A, Maxeiner J, Martin H, Yogev N, Waisman A, Gerhard M, Cover TL, Taube C, Müller A. 2014. Effective treatment of allergic airway inflammation with Helicobacter pylori immunomodulators requires BATF3-dependent dendritic cells and IL-10. Proc Natl Acad Sci U S A 111:11810–11815. https://doi.org/10.1073/pnas.1410579111.
69. Dickson RP, Singer BH, Newstead MW, Falkowski NR, Erb-Downward JR, Standiford TJ, Huffnagle GB. 2016. Enrichment of the lung microbiome with gut bacteria in sepsis and the acute respiratory distress syndrome. Nat Microbiol 1:16113. https://doi.org/10.1038/nmicrobiol.2016.113.